DYNAMIC MODEL OF A CRANKSHAFT ASSEMBLY WITH TWO DEGREES OF FREEDOM

Adrian Chmielewski, Łukasz Bogucki, Robert Gumiński, Jędrzej Mączak

Warsaw University of Technology
Faculty of Automotive and Construction Machinery Engineering
Narbutta Street 84, 02-524 Warsaw, Poland
tel.: +48 22 2348117, fax: +48 22 2348121
e-mail: a.chmielewski@mechatronika.net.pl

Abstract

Nowadays, growing attention is directed towards energy efficiency and issues related to respecting energy. An extremely vital role at improving energy efficiency plays the cogeneration technologies. In the 2012/27/UE Directive [1], the gas turbines [2] in combination with heat recovery, combustion engines [3, 4], steam engines [4], fuel cells [5-7], microturbines [8], Rankine organic cycle [9, 10], Stirling engines [11-15], and others, were included among cogeneration technologies, in which electric energy is produced from waste heat in the combined process. In this work, the distributed generation sources have also been addressed. From the perspective of the article herein, the sources equipped with the crankshaft assembly have been particularly emphasised. This mechanism converts chemical energy of, among others, fuel or working element into mechanical energy (the piston reciprocating motion is converted into rotary motion of a crankshaft).

In this work, the physical model of the crankshaft assembly has been shown, with two degrees of freedom. On the basis of analysis of the physical model (with the static mass reduction), a single-piston simulation model has been developed of the crankshaft assembly, using the Matlab&Simulink software. On the basis of the analysis of the system, the motion equations have been derived, which served the purpose of building the simulation model. Because of the conducted simulations, the curves of displacement, velocity, and piston acceleration have been presented, and, respectively, the angular displacement, angular velocity, and angular acceleration of the crankshaft. The constructed model should be seen as a part of a multi-piston working mechanism in a, for example, Stirling engine.

Keywords: Distributed generation, dynamic model, crankshaft assembly

1. Introduction

In the context of the 2020 climate package [1, 16-22], defined obligations are imposed upon the European Union member states, including: increasing the participation of renewable energy sources (RES) in the energy market to nearly 20%, improving energy efficiency (to nearly 20%) [1, 23, 24], and reducing CO_2 emissions to the atmosphere (20%). Currently, the framework of the EU energy policy is determined in the prospect of 2030 and 2050 [18]. In view of 2030 [18], the new aims have been defined, which include among others: increase of energy efficiency to 27%, increase of the RES participation to 27%, as well as reduction of CO_2 emissions to nearly 40%. The mentioned aims will have a substantial influence on the development of technologies, which in Poland will affect the competitiveness of domestic economy. The improvement of energy efficiency is seen as depending on development of the distributed generation sources [23], which denotes distributed energy production in close proximity to the places of its consumption. Decentralised energy production is characterised by lower transfer losses and system readiness to connecting new sources of energy production, which have been shown in Tab. 1 together with their power ranges. In Fig. 1, the devices have also been divided into these producing only electric energy (renewable energy sources), and the appliances working in the process of combined production of electric energy and heat in cogeneration. Depending on the size of the distributed sources, for the capacity below 150 MW [23, 25, 26], the distributed microgeneration (1 W to 5 kW), small distributed generation (5 kW do 5 MW), medium-sized distributed generation (5 MW to 50 MW), and large distributed generation (50 MW to 150 MW) can be distinguished.
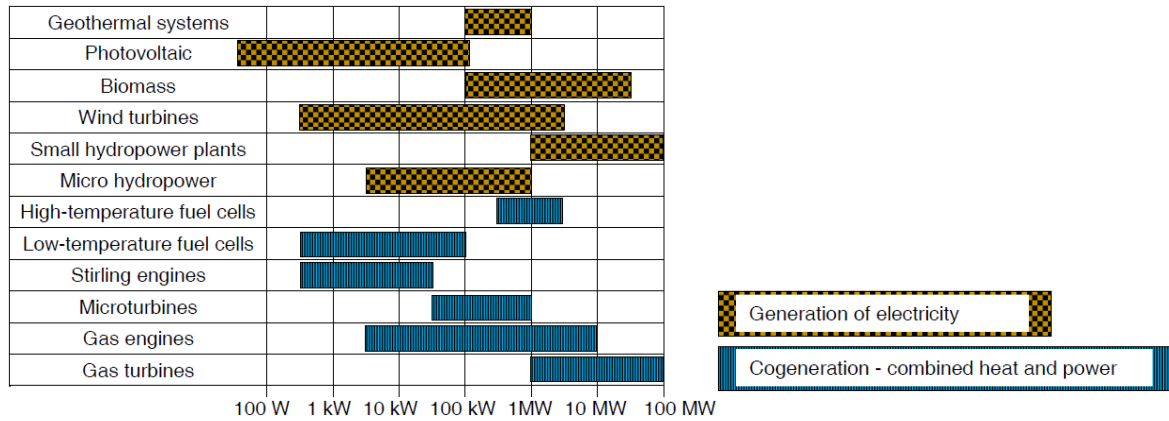
Fig. 1. Sources of distributed generation and their power ranges [23, 25, 26]

In many sources of distributed generation the change of the chemical energy form (e.g.: fuels – internal combustion engines or working element, e.g. Stirling engines) into mechanical energy takes place using working mechanisms [27]. The most frequently used mechanism in the engine domain, is a crankshaft assembly. In this work, the model of a crankshaft assembly with two degrees of freedom has been presented, where the crankshaft and the flywheel are treated as two masses with moments of inertia $I_0 = I_w + m_s r^2$ and $I_2 = I_z$ (I_w – crankshaft moment of inertia, I_0 – reduced moment of inertia of a crankshaft, I_z – flywheel moment of inertia).

2. Physical model with two degrees of freedom

In Fig. 2a, the physical model has been shown, which assumes static reduction of crankshaft masses. Similar assumptions were made in works [28, 29]. The considered physical model has two degrees of freedom. The flywheel is connected with the shaft by means of the flexible element of a rigidity k_1. The model of a real mechanism made using the reverse engineering with the help of the Solidworks software, has been shown in Fig. 2b.
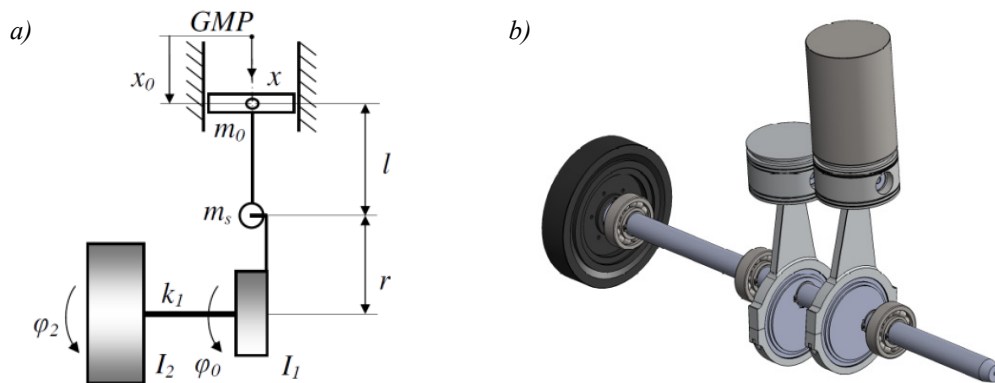

Fig. 2. Diagram of the simulated crankshaft assembly (a) and crankshaft assembly of the Alpha-type Stirling engine (b)

2.1. Theoretical basis – motion equations of the considered model

In this subchapter, the mathematical relationships have been presented, which served the purpose of building the dynamic model by means of the Matlab&Simulink software. In Fig. 3a, a diagram of the crankshaft assembly is shown, with the angles marked. A diagram of the crank mechanism is shown in Fig. 3b with the forces and moments marked.

The sum of moments relative to the TDC point (based on Fig. 2a, 3a and 3b):

$$M - I_0 \ddot{\varphi}_0 - Fr\sin(\varphi_0 + \gamma_0) - k_1(\varphi_0 - \varphi_2) = 0 \,. \tag{1}$$
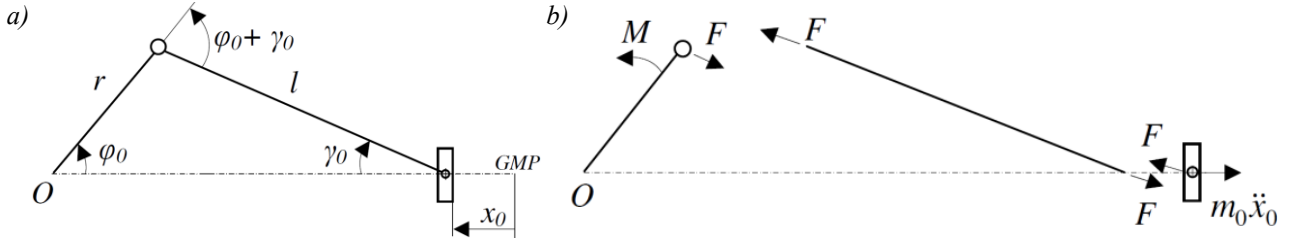
Fig. 3. Diagram of a crank mechanism: angles marked (a), forces and moment marked (b)

The sum of moments relative to the flywheel (on the basis of Fig. 2a):

$$-I_2\ddot{\varphi}_2 + k_1(\varphi_0 - \varphi_2) = 0. \tag{2}$$

The sum of forces relative to the *x*-axis (on the basis of Fig. 3a and 3b):

$$F\cos\gamma_0 - m_0\ddot{x}_0 = 0. \tag{3}$$

From the theorem of sines for an equilateral triangle, the relationship between the angle φ_0 and γ_0 is obtained:

$$\frac{l}{\sin\varphi_0} = \frac{r}{\sin\gamma_0}. \tag{4}$$

Knowing that the coefficient of the crankshaft $\lambda = r/l$, the following can be stated:

$$\cos\gamma_0 = \sqrt{1 - \frac{r^2}{l^2}\sin^2\varphi_0} = \sqrt{1 - \lambda^2\sin^2\varphi_0}. \tag{5}$$

After substituting the equations (2–5) in the equation (1), eventually the angular acceleration of the crankshaft is obtained, which was used to building the single-cylinder model of the crankshaft assembly in the Matlab&Simulink programme. The simulation results have been presented in sub-chapter 2.2.

$$\ddot{\varphi}_0 = \frac{M}{I_0} - \frac{\lambda\sin\varphi_0\cos\varphi_0 + \sin\varphi_0\sqrt{1 - \lambda^2\sin^2\varphi_0}}{\sqrt{1 - \lambda^2\sin^2\varphi_0}}\frac{r\,m_0}{I_0}\ddot{x}_0 - \frac{k_1}{I_0}(\varphi_0 - \varphi_2) = 0. \tag{6}$$

The relationship of the piston displacement x_0 calculated from the top dead centre (TDC) that is determined from the kinematic relationships shown in Fig. 2 and 3. The kinematic relationships can be written:

$$x_0 = r + l - r\cos\varphi_0 - l\cos\gamma_0. \tag{7}$$

Knowing the relationship between φ_0 and γ_0, the relationship describing the piston displacement can be written:

$$x_0 = r\left\{(1 - \cos\varphi_0) + \frac{l}{r}\left(1 - \sqrt{1 - \frac{r^2}{l^2}\sin^2\varphi_0}\right)\right\} = r\left\{(1 - \cos\varphi_0) + \frac{1}{\lambda}(1 - \sqrt{1 - \lambda^2\sin^2\varphi_0})\right\}. \tag{8}$$

After expanding the equation (8) into the infinite Taylor series and after simplification of two expressions, the following can be written:

$$x_0 = r\left\{(1 - \cos\varphi_0) + \frac{\lambda}{4}(1 - \cos 2\varphi_0)\right\}. \tag{9}$$

The piston velocity will amount to:

$$\dot{x}_0 = \frac{\mathrm{d}x_0}{\mathrm{d}t} = r\dot{\varphi}_0 \left\{ \sin\varphi_0 + \frac{\lambda}{2}\sin 2\varphi_0 \right\}. \tag{10}$$

Whereas the piston acceleration will amount:

$$\ddot{x}_0 = \frac{\mathrm{d}^2 x_0}{\mathrm{d}t^2} = r\left[\ddot{\varphi}_0\left(\sin\varphi_0 + \frac{\lambda}{2}\sin 2\varphi_0\right) + \dot{\varphi}_0^2\left(\cos\varphi_0 + \lambda\cos 2\varphi_0\right) \right]. \tag{11}$$

2.2. Simulation results

In this subchapter the input data for the simulation model has been shown, which was constructed on the basis of the derived motion equations in the subchapter 2.1. The input parameters for the simulation model have been presented in Tab. 1. These parameters were selected on the basis of the real-life Stirling engine, which is a part of the equipment at the Integrated Laboratory of Mechatronic Systems of Vehicles and Construction Machinery (Fig. 4).
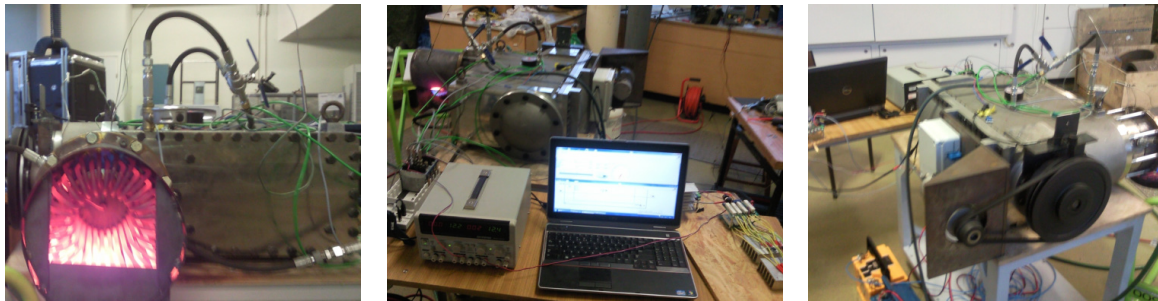

Fig. 4. Pictures of the test bench with the Alpha-type Stirling engine

It should be emphasised that the input parameters for the model have constant values. Nonlinear dynamics of the operation of the crankshaft assembly with two degrees of freedom with the abrupt torque extortion is shown in the equation (6), and the equations (9-11).

Tab. 1. Input parameters of the simulation model

Simulation model input data	
Crankshaft moment of inertia	$I_0 = 0.26$ kg·m^2
Flywheel moment of inertia	$I_2 = 0.58$ kg·m^2
Crank radius	$r = 0.06$ m
Piston mass	$m_0 = 1.1$ kg
Connecting rod length	$l = 0.26$ m
Crankshaft rigidity	$k_1 = 6500$ N·m/rad
Torque extortion	$M = 1.5$ N·m

In Fig. 5, step torque extortion has been shown (for the simulation time range 10 and 100 s). After the time $t = 1$ s the extortion torque amounts to $M = 1.5$ N·m, which has been shown in Fig. 5.

The simulation results have been shown for 10 and 100 seconds because the assembly reaches the constant value of the piston acceleration amplitude, piston velocity, and crankshaft velocity and angular acceleration no sooner than after 85 seconds. In the time range of 0-10 seconds, the assembly behaviour immediately after torsion has been shown (which is not clear for the simulation time $t = 100$ s). In Fig. 6, the change in piston displacement obtained from the model has been shown. Analysing the displacement curve enables the observation of the assembly acceleration. It should be emphasised here, that both the input parameters and the simulation parameters have a significant influence on the assembly's behaviour, including the step and simulation time. The presented results can be compared to very similar simulation results discussed in works [28, 29].
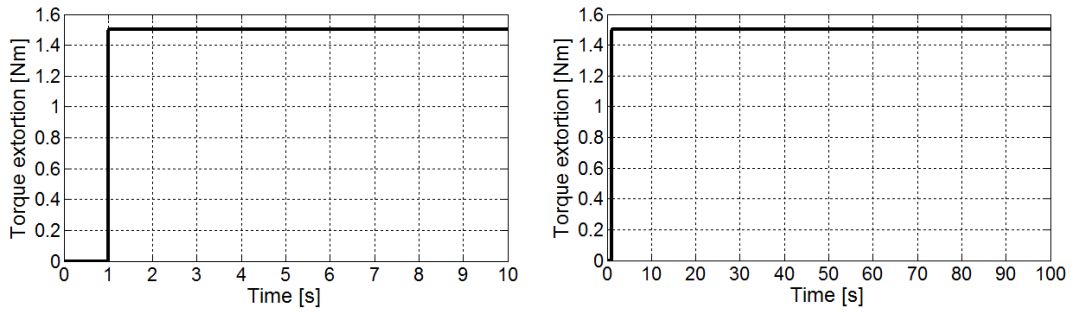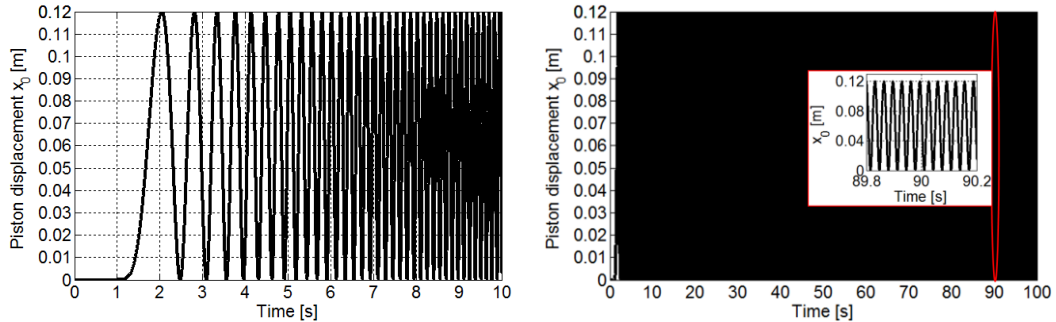
Fig. 5. Torque extortion

Fig. 6. Piston displacement

Figure 7 shows the curve of the piston velocity. The piston velocity increases – the system is accelerated to 85-90 seconds Above the 90 seconds the amplitude of velocity becomes set at a constant level. It should also be emphasised that the momentary velocity after $t = 90$ s changes sinusoidally.

The curve of the piston acceleration is also very interesting (Fig. 8). The acceleration grows up to the 90 seconds, the system speeds up. Above the 90 seconds, the acceleration amplitude reaches the constant value. From the left side (Fig. 8) it is clearly seen that the system speeds up from the 1 second (after torsion shown in Fig. 5 becomes operative).
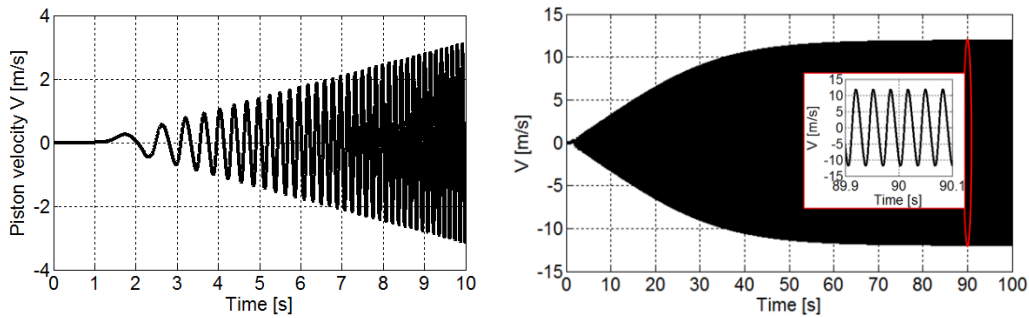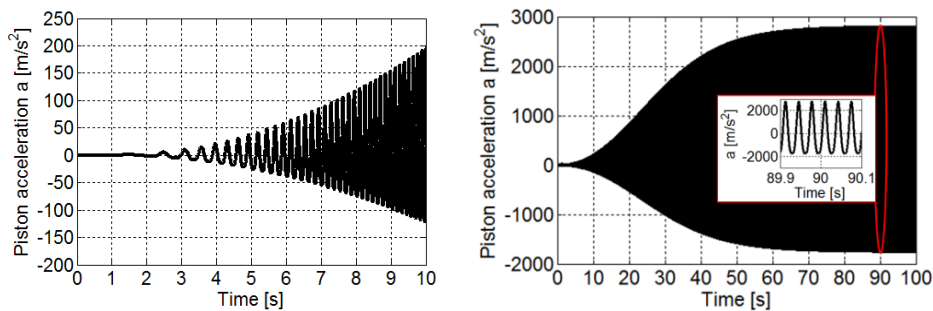

Fig. 7. Piston velocity curve

Fig. 8. Piston acceleration curve

Figure 9 shows the curve of the φ_0 angle. The curve is of nonlinear character, which proves that the system accelerates during the first stage of the simulation and then the angular displacement grows linearly (the constant angular velocity becomes set – Fig. 10).

The angular velocity grows, too (Fig. 10) from the moment $t = 1$ s, in which the torque extortion takes place (Fig. 5). After 90 seconds of simulation, the angular velocity becomes set at the level of 194 rad/s. Similar, curves of the angular velocity were presented in works [30, 31], where the model of changing system's dynamics was one of the submodels of the real-life object, in this case the Stirling engine.

Figure 11 shows the curve of the crankshaft angular acceleration. In the beginning, during torsion, at the moment of $t = 1$ s, a rapid growth of the assembly angular acceleration takes place (to 50 seconds). From 50 to 90 seconds, the acceleration amplitude increase is less rapid. Above 90 seconds, the system reaches the acceleration with the constant amplitude.

It can be concluded from the abovementioned simulation results, that in practice, for example, for cogeneration work, such a system should be loaded with a moment no sooner than after 90 seconds (within the range of a determined rotational velocity).
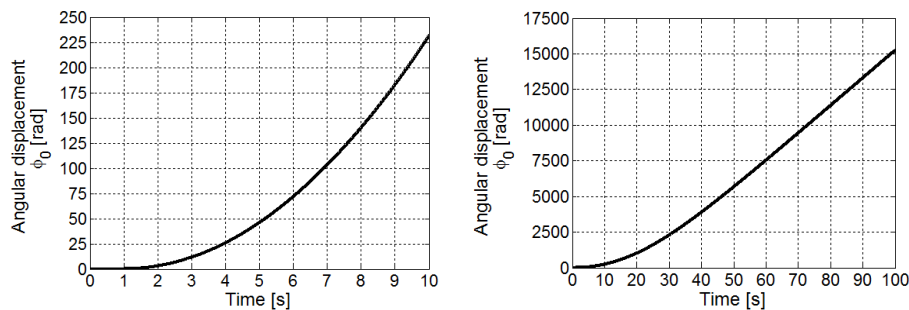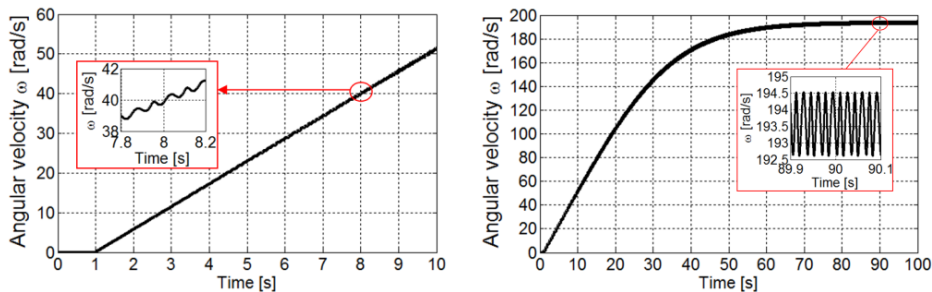
Fig. 9. Curve of the crankshaft angular displacement

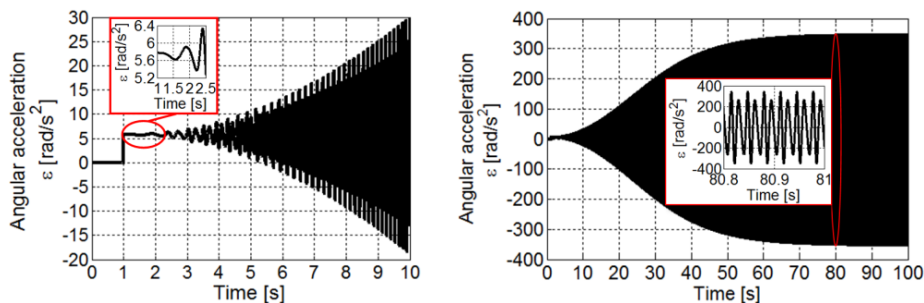*Fig. 10. The curve of the crankshaft angular velocity*

Fig. 11. Curve of the crankshaft angular acceleration

3. Summary

In this paper, the simulation model as well as the simulation results of the piston-crankshaft system with two degrees of freedom has been presented. The curves of displacement, velocity,

piston acceleration, as well as the curves of the angular displacement, angular velocity, and angular acceleration of the crankshaft have been depicted. The presented model will be extended in future to the form of a model with two pistons offset by a predetermined phase angle. Such a model will reflect the piston-crankshaft mechanism seen in the one-action, Alpha-type Stirling engine. The presented simulation results will serve the purpose of building the dynamic model of the Stirling engine including the thermodynamic processes taking place during the heat cycle. Similar works were conducted by the authors in [30]. In paper [31], the dynamic model of the Alpha-type Stirling engine has been shown, whose key element was a crankshaft assembly. The model of the changing dynamics of a crankshaft assembly has been connected with the thermodynamic model of the II order, which considers the engine's specific requirements, as well as the losses occurring in the engine [31].

List of symbols

$\lambda = r/l$ – connecting rod coefficient [–],
r – crank radius [m],
k_1 – crankshaft rigidity [N/m],
I_0 – reduced moment of crankshaft inertia [kg·m^2],
x_0 – piston displacement [m],
$v = \dot{x}_0$ –piston velocity [m/s],
$a = \ddot{x}_0$ –piston acceleration [m/s^2],
TDC – top dead centre,

φ_0 – crankshaft angular displacement [rad],
$\omega = \dot{\varphi}_0$ –crankshaft angular velocity [rad/s],,
$\varepsilon = \ddot{\varphi}_0$ –crankshaft angular acceleration [rad/s^2],
φ_2 – flywheel angular displacement [rad],
m_0 – piston mass [kg],
m_s – reduced mass on crankshaft [kg],
M – torque [N·m],
F – force [N],
$I_2 = I_z$ – flywheel moment of inertia [kg·m^2].

References

[1] Directive 2012/27/EU of the European Parliament and of the Council of 25 October 2012 *on energy efficiency, amending Directives 2009/125/EC and 2010/30/EU and repealing Directives 2004/8/EC and 2006/32/EC.*

[2] Nkoin, B., Pilidis, P., Nikolaidis, T., *Performance Assessment of Simple and Modified Cycle Turboshaft Gas Turbines*, Propulsion and Power Research, Vol. 2, No. 2, pp. 96-106, 2013.

[3] Wierzbicki, S., *Laboratory Control and Measurement System of a Dual-Fuel Compression Ignition Combustion Engine Operating in a Cogeneration System*, Solid State Phenomena, Vol. 210, pp. 200-205, 2014.

[4] Fu, J., Liu, J., Ren, C., Wang, L., Deng, B., Xu, Z., *An Open Steam Power Cycle Used for IC Engine Exhaust Gas Energy Recovery*, Energy, No. 44, pp. 544-554, 2012.

[5] Szczęśniak, A., Milewski, J., *The Reduced Order Model of a Proton–Conducting Solid Oxide Fuel Cell*, Journal of Power Technologies, Vol. 94, No. 2, pp. 122-127, 2014.

[6] Milewski, M., Discepoli, G., Desideri, U., *Modeling the Performance of MCFC for Various Fuel and Oxidant Compositions*, International Journal of Hydrogen Energy, Vol. 39, pp. 11713-11721, 2014.

[7] Stempiena, J. P., Sunc Q. H., Chan, S., *Solid Oxide Electrolyzer Cell Modeling: A Review*, Journal of Power Technologies, Vol. 93, No. 4, pp. 216-246, 2013.

[8] Ismail, M. S., Moghavemi, M., Mahlia, T. M. I., *Current Utilization of Microturbines as a Part of a Hybrid System in Distributed Generation Technology*, Renewable and Sustainable Energy Reviews, Vol. 21, pp. 142-152, 2013.

[9] Shahinfard, S., Beyene, A., *Regression Comparison of Organic Working Mediums for Low Grade Heat Recovery Operating on Rankine Cycle*, Journal of Power Technologies, Vol. 93, No. 4, pp. 257-270, 2013.

[10] Wang, T., Zhang, Y., Shu, C., *A Review of Researches on Thermal Exhaust Heat Recovery with Rankine Cycle*, Renewable and Sustainable Energy Reviews, No. 15, pp. 2862-2871, 2011.

[11] Chmielewski A., Gumiński R., Radkowski S., Szulim P., *Experimental Research and Application Possibilities of Microcogeneration System with Stirling Engine*, Journal of Power Technologies (Polish Energy Mix), pp. 1-9, 2015.

[12] Renzi, M., Brandoni, C., *Study and Application of a Regenerative Stirling Cogeneration Device Based on Biomass Combustion*, Applied Thermal Engineering, Vol. 67, pp. 341-351, 2014.

[13] Xiao, G., Chen, C., Shi, B., Cen, K., Ni, M., *Experimental Study on Heat Transfer of Oscillating Flow of a Tubular Stirling Engine Heater*, International Journal of Heat and Mass Transfer, Vol. 71, pp. 1-7, 2014.

[14] Cheng, C. H., Yang, H. S., Keong, L., *Theoretical and Experimental Study of a 300W Beta–Type Stirling Engine*, Energy, Vol. 59, pp. 590-599, 2013.

[15] Li, T., Tang, D., W., Li, Z., Du, J., Zhou, T., Jia, Y., *Development and Test of a Stirling Engine Driven by Waste Gases for the Micro–CHP System*, Applied Thermal Engineering Vol. 33-34, pp. 119-123, 2012.

[16] Directive 2009/28/EC of the council of 23 april 2009, *on the promotion of the use of energy from renewable sources and amending and subsequently repealing Directives 2001/77/EC and 2003/30/EC.*

[17] Directive 2004/8/EC of the European Parliament and of the council of 11 February 2004 *on the promotion of cogeneration based on a useful heat demand in the internal energy market and amending Directive 92/42/EC.*

[18] CO EUR 13 CONCL 5, *Ramy polityki klimatyczno-energetycznej do roku 2030*, Bruksela 24 października 2014.

[19] Chmielewski A., Radkowski S., *Prosumer on the Energy Market: Case Study*, Proceedings of the Institute of Vehicles, 2(102)/2015 [in print].

[20] Chmielewski A., Radkowski S., *Rozwój odnawialnych źródeł energii na terenie Polski – wyzwania i problemy*, Zeszyty Naukowe Instytutu Pojazdów, 3(99), s. 13-24, 2014.

[21] Kim, J. D., Rahimi, M., *Future Energy Loads for a Large-Scale Adoption of Electric Vehicles in the City of Los Angeles: Impacts on Greenhouse Gas (GHG) Emissions*, Energy Policy, Vol. 73, pp. 620-630, 2014.

[22] Chmielewski, A., Radkowski S., *Smart grid jako jeden z elementów poprawy efektywności energetycznej Polski w perspektywie 2020*, Zeszyty Naukowe Instytutu Pojazdów, 3(99), s. 25-34, 2014.

[23] Chmielewski, A., Gumiński, R., Radkowski S., Szulim P., *Aspekty wsparcia i rozwoju mikro-kogeneracji rozproszonej na terenie Polski*, Rynek Energii, Nr 5 (114), s. 94-101, 2014.

[24] Chmielewski, A., Lubikowski, K., Radkowski, S., *Simulation of Energy Storage Work and Analysis of Cooperation Between Micro Combined Heat and Power (μCHP) Systems and Energy Storage*, Rynek Energii, Nr 5 (117), pp. 126-133, 2015.

[25] Instytut energii odnawialnej, *Energetyka rozproszona*, Fundacja Instytut na rzecz Ekorozwoju, Warszawa 2011.

[26] Szczerbowski, R., Chomicz, W., *Generacja rozproszona oraz sieci Smart Grid w budownictwie przemysłowym niskoenergetycznym*, Polityka Energetyczna, T. 15, Z. 4, 2012.

[27] Loth, E., Dobrzyński, S., Bernhardt, M., *Silniki samochodowe*, WKiŁ, 1988.

[28] Jankowski, A., Jeż, M., Świder, A., *Investigation of Non-Linear Dynamics of Crankshaft Assembly*, Journal of KONES, Vol. 5, No. 1-2, pp. 217-227, 2000.

[29] Jeż, M., Świder, A., *Analiza drgań nieliniowych jednocylindrowego silnika tłokowego*, Journal of KONES, Vol. 8, No. 3-4, pp. 98-105, 2001.

[30] Cheng, C., H., Yang, H. S., Jhou, B. Y., Chen, Y. C., Wang, Y. J., *Dynamic Simulation of Thermal–Lag Stirling Engines*, Applied Energy, Vol. 108, pp. 466-476, 2013.

[31] Scollo, L. S., Valdez, P. E., Santamarina, S. R., Chini, M. R., Baron, J. H., *Twin Cylinder Alpha Stirling Engine Combined Model and Prototype Redesign*, International Journal of Hydrogen Energy, Vol. 38, pp. 1988-1996, 2013.